Eur. Phys. J. C 20, 553–562 (2001)
Digital Object Identifier (DOI) 10.1007/s100520100691

THE EUROPEAN PHYSICAL JOURNAL C

R_b and R_ℓ in MSSM without R-parity

J.M. Yang

Institute of Theoretical Physics, Academia Sinica, Beijing 100080, P.R. China

Received: 14 October 1999 / Revised version: 2 May 2001 /
Published online: 8 June 2001 – © Springer-Verlag / Società Italiana di Fisica 2001

Abstract. We examined $Zb\bar{b}$ and $Z\ell\bar{\ell}$ couplings in the minimal supersymmetric model with explicit trilinear R-parity violating interactions. We found that the top quark couplings λ'_{i3k} and λ''_{3j3} can give sizable contributions through top quark loops. When deriving the bounds from R_b and R_ℓ data, we also take into account the loop contributions of R-parity conserving interactions. The bounds from R_ℓ are found to be stronger than those from R_b and serve as the hitherto strongest bounds for some couplings.

1 Introduction

The standard model (SM) has been very successful phenomenologically. Yet, despite its success, the SM is still believed to be a theory effective at the electroweak scale while new physics must exist at higher energy regimes. Some approaches have been developed to describe such new physics, such as the model-independent effective Lagrangian approach [1] and various new models. Among the new models the weak-scale minimal supersymmetric model (MSSM) [2] has many attractive features and is arguably the most promising one.

In the MSSM, the invariance of R-parity, defined by $R = (-1)^{2S+3B+L}$ for a field with spin S, baryon number B and lepton number L, is often imposed on the Lagrangian in order to maintain the separate conservation of baryon number and lepton number. However, this conservation is not dictated by any fundamental principle such as gauge invariance and there is no compelling theoretical motivation for it. The most general superpotential of the MSSM consistent with the $SU(3) \times SU(2) \times U(1)$ symmetry and supersymmetry contains R violating ($\not{R}$) interactions which are given by [3]

$$\mathcal{W}_{\not{R}} = \frac{1}{2}\lambda_{ijk} L_i L_j E^c_k + \lambda'_{ijk} L_i Q_j D^c_k + \frac{1}{2}\lambda''_{ijk}\epsilon^{abd} U^c_{ia} D^c_{jb} D^c_{kd} + \mu_i L_i H_2, \qquad (1.1)$$

where $L_i(Q_i)$ and $E_i(U_i, D_i)$ are the left-handed lepton (quark) doublet and right-handed lepton (quark) singlet chiral superfields. i, j, k are generation indices and c denotes charge conjugation. a, b and d are the color indices and ϵ^{abd} is the totally antisymmetric tensor. $H_{1,2}$ are the Higgs doublet chiral superfields. The λ_{ijk} and λ'_{ijk} are L violating ($\not{L}$) couplings, λ''_{ijk} B violating ($\not{B}$) couplings. λ_{ijk} is antisymmetric in the first two indices and λ''_{ijk} is antisymmetric in the last two indices. The phenomenological studies for these $\not{R}$ couplings were started a long time ago [3]. While this is an interesting problem in its own right, the recent anomalous events at HERA [4] and the evidence of neutrino oscillations [5] might provide an additional motivation for the study of these $\not{R}$ couplings. So both theorists and experimentalists have recently intensively examined the phenomenology of R-parity breaking supersymmetry in various processes [6,7] and obtained some bounds [8].

Some of these $\not{R}$ couplings contribute to the precisely measured $Zb\bar{b}$ and $Z\ell\bar{\ell}$ couplings through sfermion–fermion loops. Since the MSSM is a renormalizable field theory and the sparticles get their masses through explicit soft breaking terms, the decoupling theorem [9] implies that the effects of these sparticle loops will be suppressed by some orders of $1/M_{\rm SUSY}$ and vanish as $M_{\rm SUSY}$ goes far above the weak scale. So, in general, these sfermion–fermion loop effects on lower energy observables are small. However, due to the non-decoupling property of heavy SM particles (which get masses through spontaneous gauge symmetry breaking), the effects of the sfermion–fermion loops involving the top quark (hereafter called the top quark loops) may be enhanced by the large top quark mass. Therefore, the $\not{R}$ top quark couplings in (1.1), λ'_{i3k} and λ''_{3jk}, which currently are subject to quite weak bounds (see [8] for a review), may give rise to significant contributions through the top quark loops.

Although some bounds on the $\not{R}$ couplings were derived from $R_\ell \equiv \Gamma(Z \to \text{hadrons})/\Gamma(Z \to \ell\bar{\ell})$ a few years ago [10], it is necessary to give a thorough examination of the $\not{R}$ quantum effects on the $Zb\bar{b}$ and $Z\ell\bar{\ell}$ couplings since the measurements of both $R_b \equiv \Gamma(Z \to b\bar{b})/\Gamma(Z \to \text{hadrons})$ and R_ℓ have been much improved nowadays [11]. Also, when deriving bounds from R_b and R_ℓ, the R conserving MSSM quantum effects, which were neglected in those previous studies [10], should be included.

In this paper we study the contributions of the trilinear explicit $\not{R}$ interactions to $Zb\bar{b}$ and $Z\ell\bar{\ell}$ couplings. By using the latest data of R_b and R_ℓ, we examine the

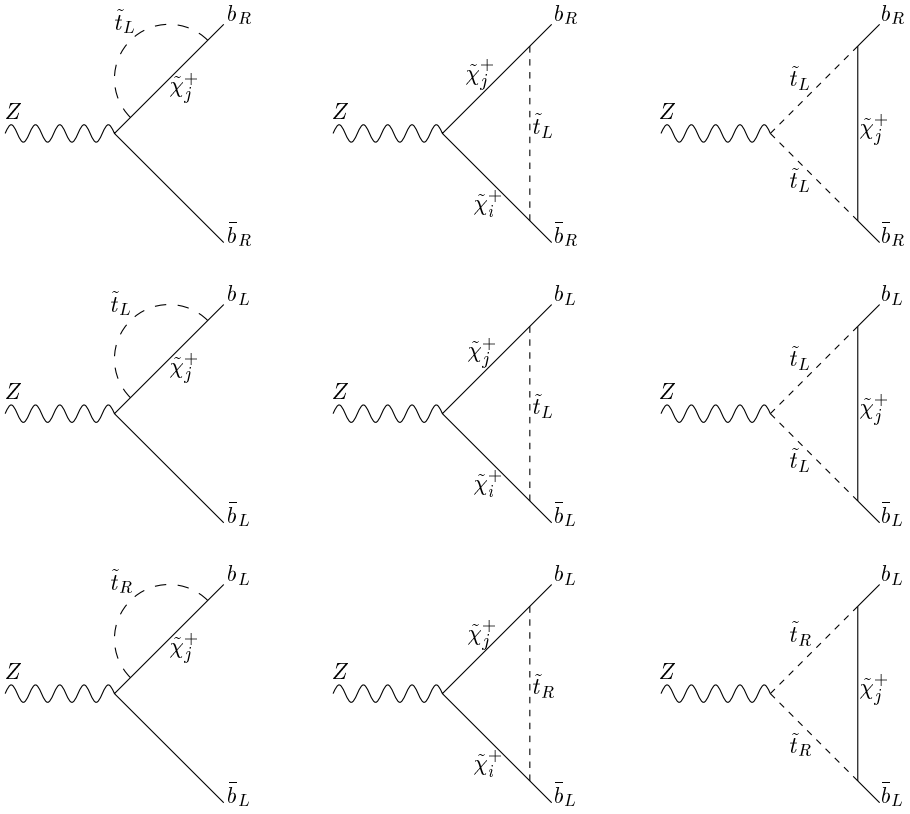

Fig. 1. Feynman diagrams of chargino-stop loops which contribute to the $Zb\bar{b}$ vertex

bounds on the top quark $\not{R}$ couplings. The R conserving MSSM quantum effects on the $Zb\bar{b}$ vertex are also taken into account in our analyses.

Note that at the level of the superpotential, the explicit $\not{L}$ terms $\mu_i L_i H_2$ can be rotated away by a field redefinition [3]. However, such a redefinition does not leave the full Lagrangian invariant when including the soft breaking terms [12]. We focus in this paper on the trilinear explicit $\not{R}$ interactions and ignore the effects of the terms $\mu_i L_i H_2$.

This paper is organized as follows. In Sect. 2 we calculate the contributions of the $\not{R}$ MSSM to $Zb\bar{b}$ and $Z\ell\bar{\ell}$ couplings. In Sect. 3 we present the contributions of the top quark couplings to R_b and R_ℓ, and derive the limits from the latest experimental data. Finally, we give the conclusions in Sect. 4.

2 $Zb\bar{b}$ and $Z\ell\bar{\ell}$ couplings in $\not{R}$ SUSY

Neglecting the dipole-moment coupling which are suppressed by m_b/m_Z, the $\not{R}$ MSSM contribution to the $Zb\bar{b}$ vertex takes the form

$$\Delta V_{Zb\bar{b}} = \mathrm{i}\frac{e}{s_{\mathrm{W}}c_{\mathrm{W}}}\gamma_\mu \left[P_R g_R^b \Delta_R^b + P_L g_L^b \Delta_L^b\right], \quad (2.1)$$

where $P_{R,L} = (1\pm\gamma_5)/2$ and g_L^b (g_R^b) is the $Zb_L\bar{b}_L$ ($Zb_R\bar{b}_R$) coupling in the SM. (Throughout this paper the subscripts R and L stand for chirality.) The new physics contribution factors Δ_L^b and Δ_R^b contain both the R conserving MSSM contribution and $\not{R}$ contribution which are denoted by

$$\Delta_L^b = \Delta_L^{(\mathrm{MSSM})} + \Delta_L^{(\not{R})}, \quad (2.2)$$

$$\Delta_R^b = \Delta_R^{(\mathrm{MSSM})} + \Delta_R^{(\not{R})}. \quad (2.3)$$

The R conserving MSSM interactions contribute to R_b mainly through [13]:

(1) Chargino–stop loops. Their contribution is most likely sizable since they contain the large $\tilde{t}_R$–b_L–Higgsino Yukawa coupling squared, which is proportional to $(M_t^2/M_{\mathrm{W}}^2)(1+\cot^2\beta)$.

(2) Charged and neutral Higgs loops. For a very light CP-odd Higgs boson A^0 ($50 \sim 80\,\mathrm{GeV}$) and very large $\tan\beta$ (~ 50), their contribution could be sizable [13].

(3) Neutralino–sbottom loops. Their contribution is negligibly small for low and intermediate $\tan\beta$, but could be sizable for very large $\tan\beta$ [13].

Since the dominant MSSM contribution is from the chargino–stop loops for low and intermediate $\tan\beta$ ($1 \sim 30$), we in our calculation consider the chargino–stop loops. A detailed calculation of the full one-loop effects of MSSM on $Zb\bar{b}$ coupling can be found in [13]. Here we present the results for the chargino loops.

The Feynman diagrams for chargino–stop loops are shown in Fig. 1. The contribution factor $\Delta_R^{(\mathrm{MSSM})} \equiv \Delta_R^{(\tilde{t}_L)}$ arise from the first three diagrams of Fig. 1 induced by $\tilde{t}_L$–b_R–$\tilde{\chi}_j^+$ Yukawa couplings, while $\Delta_L^{(\mathrm{MSSM})} \equiv \Delta_L^{(\tilde{t}_L)} + \Delta_L^{(\tilde{t}_R)}$ with $\Delta_L^{(\tilde{t}_L)}$ is arising from the middle three diagrams of Fig. 1, induced by $\tilde{t}_L$–b_L–$\tilde{\chi}_j^+$ gauge couplings and $\Delta_L^{(\tilde{t}_R)}$ from the last three diagrams of Fig. 1, induced by $\tilde{t}_R$–b_L–

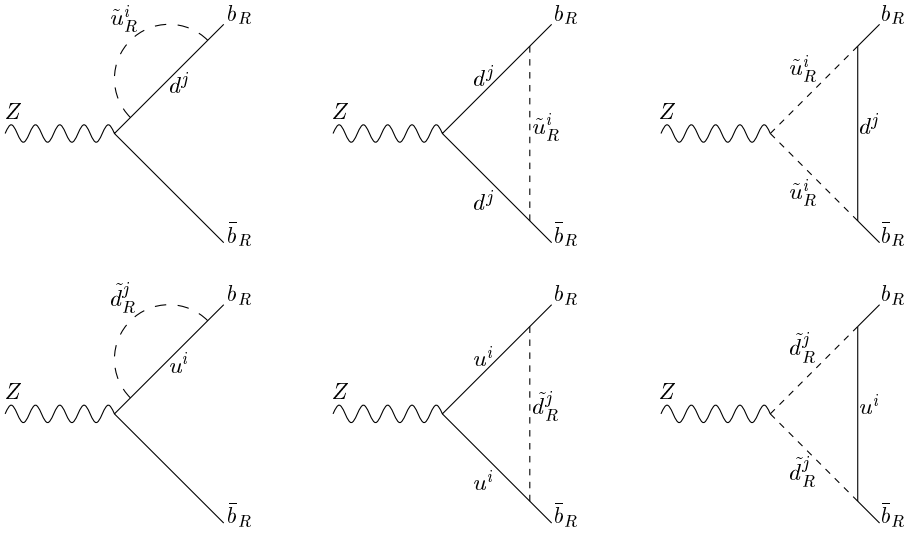

Fig. 2. Feynman diagrams for the $\not{R}$ λ''_{ij3} contributions to the $Zb_R\bar{b}_R$ vertex. i and j are flavor indices, with i = 1,2 or 3 and j = 1 or 2

$\tilde{\chi}^+_j$ Yukawa couplings. The expressions of $\Delta_R^{(\tilde{t}_L)}$, $\Delta_L^{(\tilde{t}_L)}$ and $\Delta_L^{(\tilde{t}_R)}$ are presented in the appendix.

Through loop diagrams, the $\not{R}$ couplings λ''_{ij3} and λ'_{ij3} contribute to $Zb_R\bar{b}_R$, and λ'_{i3k} contribute to $Zb_L\bar{b}_L$. (Note that, for example, λ''_{ij3} can also induce $Zb_L\bar{b}_L$ coupling through loops, which is suppressed by M_b^2/M_Z^2 and thus is negligibly small.) The Feynman diagrams for the loop contributions of these couplings to the $Zb\bar{b}$ coupling are shown in Figs. 2, 3 and 4, respectively. Their contributions, denoted $\Delta_R^{(\lambda''_{ij3})}$, $\Delta_R^{(\lambda'_{ij3})}$, and $\Delta_L^{(\lambda'_{i3k})}$ are presented in the appendix.

Also through loops, the couplings λ_{ijk} and λ'_{ijk} with i = 1, 2 and 3 contribute to $Z\ell^i\bar{\ell}^i$ with $\ell^i = e$, μ and τ, respectively. The pure leptonic couplings λ_{ijk} are not relevant to the top quark and will not be considered in our analyses. The Feynman diagrams of the contribution of λ'_{ijk} to $Z\ell^i_L\bar{\ell}^i_L$ are shown in Fig. 5. (The loops of λ'_{ijk} can also induce the $Z\ell_R\bar{\ell}_R$ coupling, which is suppressed by M_ℓ^2/M_Z^2 and thus is negligibly small.) The contribution to the $Z\ell^i\bar{\ell}^i$ vertex takes the form

$$\Delta V_{Z\ell\bar{\ell}} = \mathrm{i}\frac{e}{s_{\mathrm{W}}c_{\mathrm{W}}}\gamma_\mu\left[P_R g_R^e \Delta_R^\ell + P_L g_L^e \Delta_L^\ell\right], \quad (2.4)$$

where g_L^e and g_R^e are the couplings in the SM, and Δ_L^ℓ and Δ_R^ℓ the contributions from the couplings λ'_{ijk} with $\Delta_R^\ell \approx 0$ and Δ_L^ℓ being obtained from $\Delta_L^{(\lambda'_{i3k})}$ with substitutions of $b \to \ell$, $\nu^i \to u^j$ and $\tilde{\nu}^i \to \tilde{u}^j$.

We would like to make a few comments on our calculations.

(1) We used dimensional regularization to control the ultraviolet divergences in the virtual loop corrections and we adopted the on-mass-shell renormalization scheme. The ultraviolet divergences in the self-energy and the vertex loops are contained in Feynman integrals. We have checked that in our results, the ultraviolet divergences cancelled as a result of the renormalizability of the MSSM.

(2) Several sfermion states are involved in our calculations. In general there exists a mixing between left- and right-handed sfermions of each flavor [14]. (We do not consider the flavor mixing of sfermions.) So $\tilde{f}_{L,R}$ are in general not the physical states (mass eigenstates); instead, they are related to the mass eigenstates $\tilde{f}_{1,2}$ by a unitary rotation. In our calculations, we explicitly presented the analytical expression in terms of $\tilde{f}_{L,R}$, which can easily be translated into an expression in terms of $\tilde{f}_{1,2}$ by using the unitary relation between $\tilde{f}_{L,R}$ and $\tilde{f}_{1,2}$.

(3) We neglected the R conserving MSSM contribution to the $Z\ell\bar{\ell}$ couplings because they are expected to be small, unlike the the $Zb\bar{b}$ case where chargino–stop loops could contribute significantly.

(4) While it is theoretically possible to have both $\not{B}$ and $\not{L}$ terms in the Lagrangian, the non-observation of proton decay imposes very stringent conditions on their simultaneous presence. In our calculation (and in the following numerical calculations) we consider the presence of one non-zero coupling at one time.

In order to find out which couplings could give sizable contributions, we first perform a test numerical calculation by assuming a common mass of 100 GeV for all sparticles.

For the contributions of $\not{R}$ couplings, as expected, we found that only the top quark couplings could give sizable contributions, i.e., λ''_{3j3} and λ'_{i33} contribute significantly to $Zb\bar{b}$, while λ'_{i3k} to $Z\ell^i\bar{\ell}^i$. In each case, the dominant contribution was found to arise from the top quark loops.

For the contribution from R conserving MSSM, we found $\Delta_L^{(\tilde{t}_R)}$ is large because it is proportional to $(M_t^2/M_{\mathrm{W}}^2)(1+\cot^2\beta)$. For large $\tan\beta$, $\Delta_R^{(\tilde{t}_L)}$ also becomes sizable because it is enhanced by the factor $(M_b^2/M_{\mathrm{W}}^2)(1+\tan^2\beta)$. $\Delta_L^{(\tilde{t}_L)}$ arises from the gauge coupling and is found to be always small. We realize that although the magnitude of $\Delta_R^{(\tilde{t}_L)}$ becomes comparable to that of $\Delta_L^{(\tilde{t}_R)}$ for large $\tan\beta$, its contribution to R_b is suppressed by the factor $(g_R^b/g_L^b)^2 \approx 1/30$ relative to the contribution of $\Delta_L^{(\tilde{t}_R)}$. So, the MSSM contributions are dominated by the last three diagrams of Fig. 1, which are induced by the $\tilde{t}_R$–

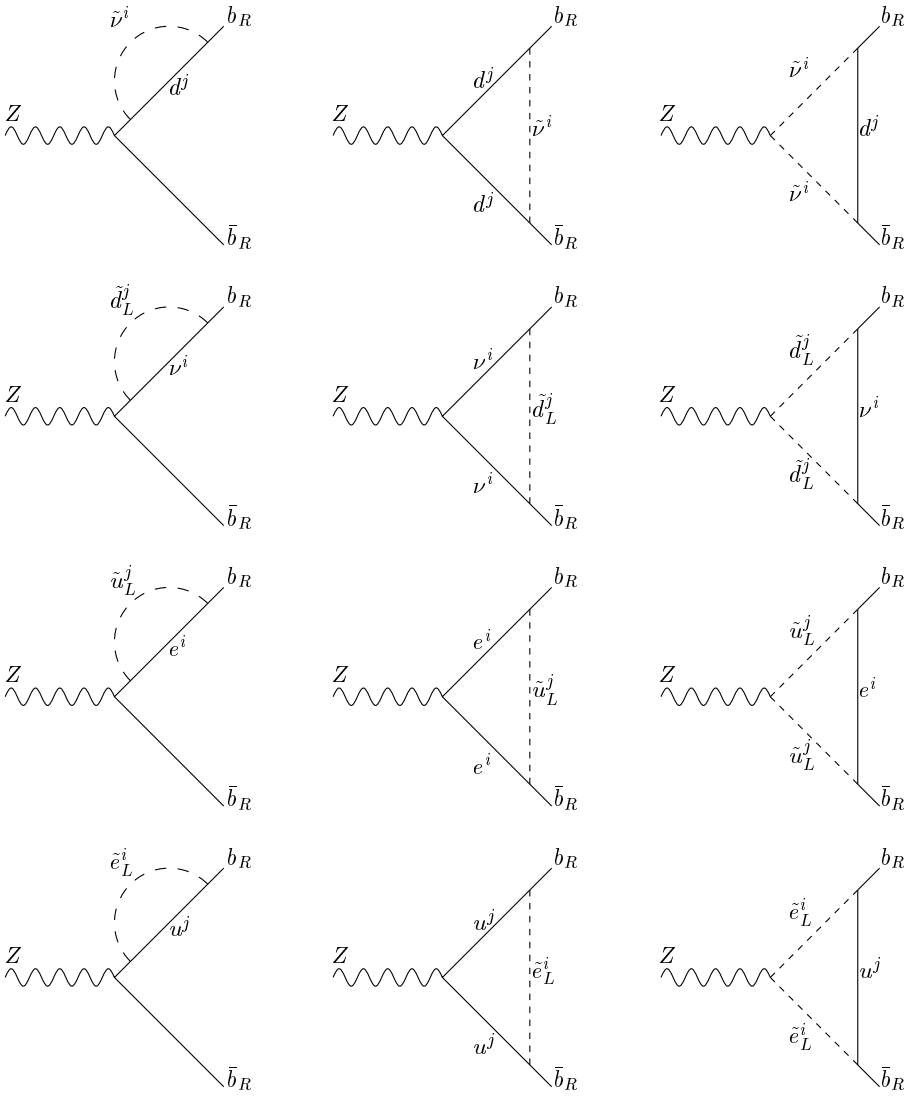

Fig. 3. Feynman diagrams for the $\not{L}$ λ'_{ij3} contributions to the $Zb_R\bar{b}_R$ vertex. i and j are flavor indices

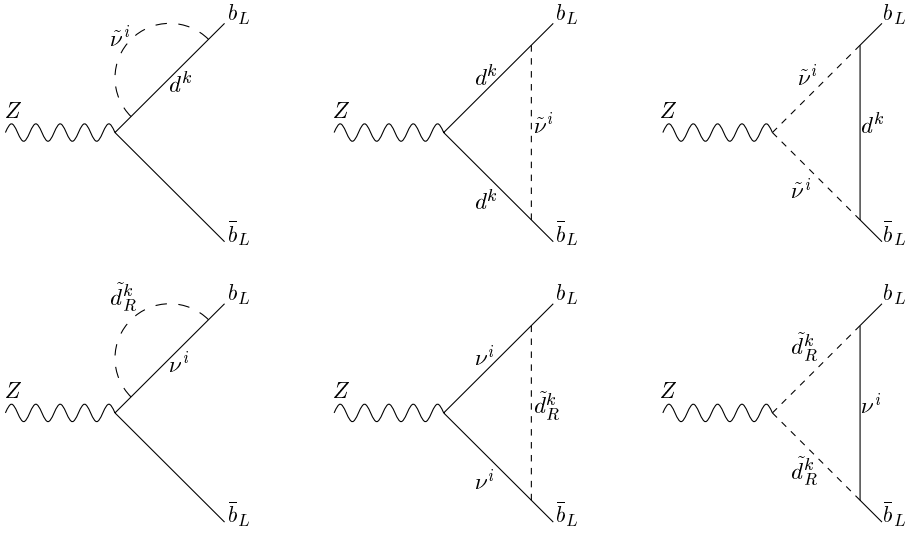

Fig. 4. Feynman diagrams for the $\not{L}$ λ'_{i3k} contributions to the $Zb_L\bar{b}_L$ vertex. i and k are flavor indices

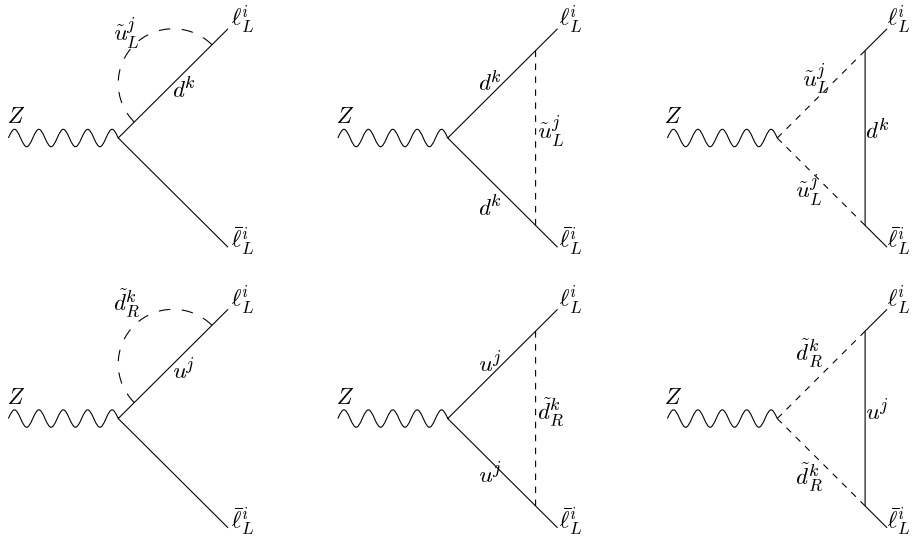

Fig. 5. Feynman diagrams for the $\not{L}$ λ'_{i3k} contributions to the left-handed $Z\ell_L\ell_L$ vertex. i and k are flavor indices

b_L–Higgsino Yukawa coupling. Such contributions, proportional to $(M_t^2/M_{\rm W}^2)(1+\cot^2\beta)$, are not sensitive to $\tan\beta$ for intermediate or large $\tan\beta$ values, but would be enhanced in the favorable scenario: (1) The lightest chargino is Higgsino-like, and (2) when the mixing of stops is considered, the lightest stop $\tilde{t}_1$ is $\tilde{t}_R$-like (the mixing angle $\theta_{\tilde{t}}$ is large).

3 The contributions of $\not{R}$ top quark couplings to R_b and R_ℓ

As found in the preceding section, only top quark couplings (λ''_{3j3} and λ'_{i3k}) can give sizable contributions to the $Zb\bar{b}$ and $Z\ell\bar{\ell}$ couplings through top quark loops. In this section we evaluate the contributions of these top quark couplings to R_b and R_ℓ and derive the bounds on the couplings. In our analysis we only keep the contributions of top quark loops. Note that we do not use the $b\bar{b}$ forward–backward asymmetry A_b to constrain the $\not{R}$ couplings. The data [11] $A_b^{\rm exp}=0.911\pm0.025$ and $A_b^{\rm SM}=0.935$ are subject to a larger error than R_b and R_ℓ.

Before presenting the results, a discussion is due regarding the SUSY parameters involved. In addition to the $\not{R}$ couplings themselves, the following SUSY parameters are involved.

(1) The R conserving contributions involve the masses and couplings of charginos, which are determined by the parameters M, μ and $\tan\beta$. M is the $SU(2)$ gaugino mass, μ is the Higgs mixing term ($\mu H_1 H_2$) in the superpotential and $\tan\beta = v_2/v_1$ is the ratio of the vacuum expectation values of the two Higgs doublets. The LEP experiments disfavored small $\tan\beta$ values [15]. The SUSY explanation of the recently reported value of the muon anomalous magnetic moment also requires a large $\tan\beta$ and a positive μ [16]. In our calculation we choose the following representative set of values:

$$M=300\,{\rm GeV}, \mu=150\,{\rm GeV}, \tan\beta=10, \qquad (3.1)$$

which yield the chargino masses as $m_{\tilde{\chi}_1^+}=133\,{\rm GeV}$ and $m_{\tilde{\chi}_2^+}=328\,{\rm GeV}$.

(2) The masses of some squarks and sleptons are involved. For each flavor of sfermion, the mass eigenstates $\tilde{f}_{1,2}$ are related to the left- and right-handed states by a unitary rotation:

$$\begin{pmatrix}\tilde{f}_L\\ \tilde{f}_R\end{pmatrix}=\begin{pmatrix}\cos\theta_{\tilde{f}} & -\sin\theta_{\tilde{f}}\\ \sin\theta_{\tilde{f}} & \cos\theta_{\tilde{f}}\end{pmatrix}\begin{pmatrix}\tilde{f}_1\\ \tilde{f}_2\end{pmatrix}, \qquad (3.2)$$

where the mixing angle $\theta_{\tilde{f}}$ and masses $m_{\tilde{f}_1}$ and $m_{\tilde{f}_2}$ are determined by the mass matrix of the sfermion. Since the off-diagonal terms in the mass matrix are proportional to the mass of the corresponding fermion [14], the mixings of sleptons and the first two generation squarks are relatively small. But for the third generation squarks, i.e., stops and sbottoms, the mixings could be significant. In our calculation we consider the mixings of stops and sbottoms. For other sfermions we neglect the mixings and, for simplicity, assume a common value for their masses. The mass matrix for stops and sbottoms are given by [14] (see (3.3) and (3.4) on top of the next page) where $s_{\rm W}\equiv\sin\theta_{\rm W}$. $\tilde{M}_Q^2$, $\tilde{M}_U^2$ and $\tilde{M}_D^2$ are the soft breaking mass terms for the left-handed and right-handed squarks. $A_t\tilde{M}$ and $A_b\tilde{M}$ are the coefficients of the dimension-three soft breaking terms proportional to the superpotential. As an illustrative example we set both A_t and A_b to unity, and

$$\tilde{M}_Q=\tilde{M}_U=\tilde{M}_D=\tilde{M}=150\,{\rm GeV}, \qquad (3.5)$$

which yields the spectrum

$$\begin{aligned} &m_{\tilde{t}_1}=149\,{\rm GeV}, m_{\tilde{t}_2}=283\,{\rm GeV},\\ &m_{\tilde{b}_1}=129\,{\rm GeV}, m_{\tilde{b}_2}=180\,{\rm GeV},\\ &\theta_{\tilde{t}}\simeq-44^\circ, \theta_{\tilde{b}}\simeq 40^\circ. \end{aligned} \qquad (3.6)$$

For the SUSY parameter values specified above, we further fix the slepton mass at 150 GeV and plot the combined effects of R conserving and $\not{R}$ couplings in Figs. 6–10. Also plotted are the experimental bounds, which are obtained from the data [11]:

$$M_{\tilde{t}}^2 = \begin{pmatrix} \tilde{M}_Q^2 + m_Z^2 \cos(2\beta)\left(\frac{1}{2} - \frac{2}{3}s_{\rm W}^2\right) + m_t^2 & m_t(A_t\tilde{M} + \mu\cot\beta) \\ m_t(A_t\tilde{M} + \mu\cot\beta) & \tilde{M}_U^2 + m_Z^2\cos(2\beta)\frac{2}{3}s_{\rm W}^2 + m_t^2 \end{pmatrix}, \tag{3.3}$$

$$M_{\tilde{b}}^2 = \begin{pmatrix} \tilde{M}_Q^2 + m_Z^2 \cos(2\beta)\left(-\frac{1}{2} + \frac{1}{3}s_{\rm W}^2\right) + m_b^2 & m_b(A_b\tilde{M} + \mu\tan\beta) \\ m_b(A_b\tilde{M} + \mu\tan\beta) & \tilde{M}_D^2 - m_Z^2\cos(2\beta)\frac{s_{\rm W}^2}{3} + m_b^2 \end{pmatrix}, \tag{3.4}$$

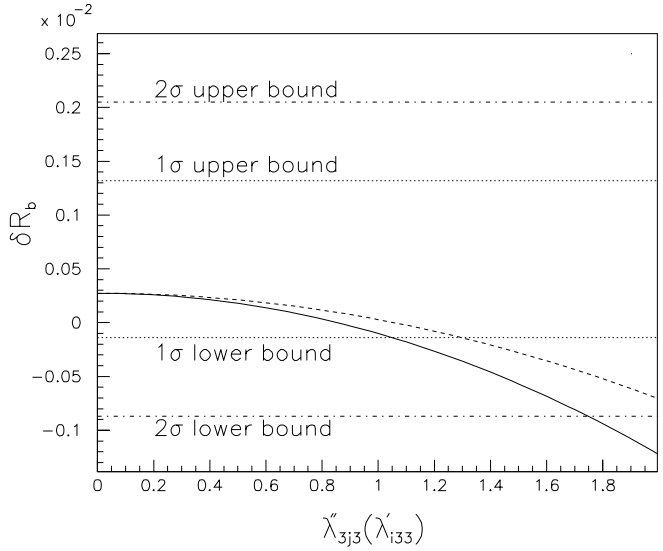

Fig. 6. δR_b versus coupling strength. The solid curve is for λ''_{3j3} ($j = 1$ or 2). The dashed curve is for λ'_{i33} ($i = 1, 2$ or 3)

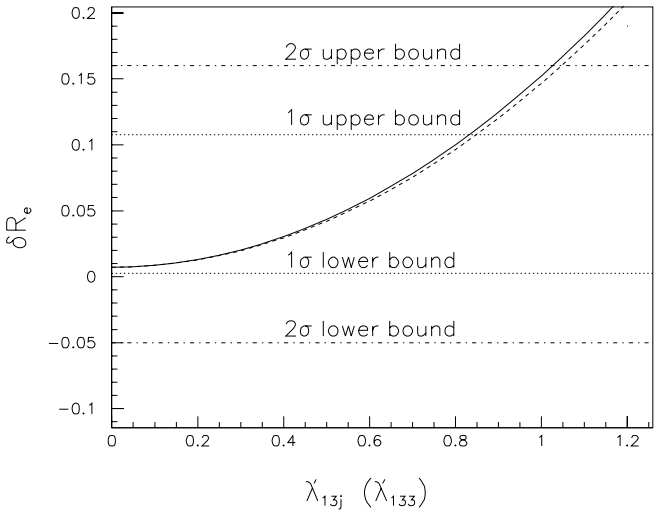

Fig. 8. δR_e versus coupling strength. The solid curve is for λ'_{13j} ($j = 1$ or 2). The dashed curve is for λ'_{133}

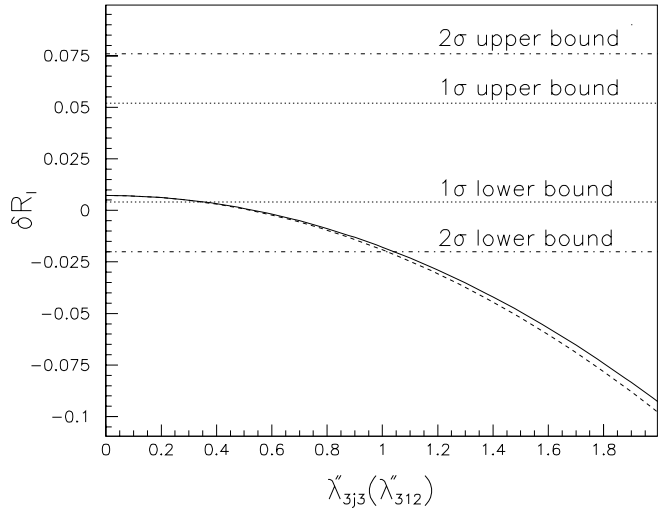

Fig. 7. δR_ℓ versus coupling strength. The solid curve is for λ''_{3j3} ($j = 1$ or 2). The dashed curve is for λ''_{312}

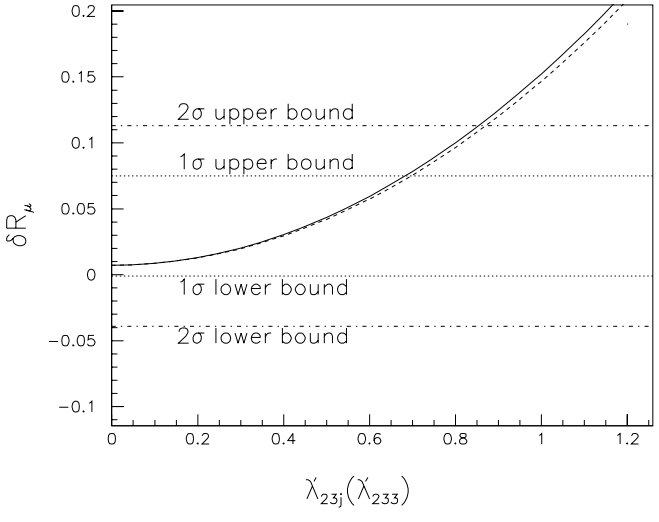

Fig. 9. δR_μ versus coupling strength. The solid curve is for λ'_{23j} ($j = 1$ or 2). The dashed curve is for λ'_{233}

$$\begin{aligned}
&R_b^{\rm exp} = 0.21642 \pm 0.00073, \quad R_b^{\rm SM} = 0.21583 \pm 0.0002,\\
&R_\ell^{\rm exp} = 20.768 \pm 0.024, \quad R_\ell^{\rm SM} = 20.740,\\
&R_e^{\rm exp} = 20.803 \pm 0.049, \quad R_e^{\rm SM} = 20.748 \pm 0.019,\\
&R_\mu^{\rm exp} = 20.786 \pm 0.033, \quad R_\mu^{\rm SM} = 20.749 \pm 0.019,\\
&R_\tau^{\rm exp} = 20.764 \pm 0.045, \quad R_\tau^{\rm SM} = 20.794 \pm 0.019,
\end{aligned} \tag{3.7}$$

where leptonic universality is assumed for R_ℓ.

As Figs. 6–10 showed, the R conserving loop contributions $\Delta R_b^{(\rm MSSM)}$ and $\Delta R_\ell^{(\lambda'_{i3k})}$ are both positive. The contributions of λ'_{i3k} to R_{ℓ^i}, as shown in Figs. 8–10, are also positive. On the contrary, the contributions of λ''_{3j3} and λ'_{i33} to R_b, as shown in Fig. 6, and the contributions of λ''_{3jk} to R_ℓ, as shown in Fig. 7, are negative.

From the figures one sees that the bounds from R_ℓ are stronger than from R_b. We vary the slepton mass and list the bounds from R_ℓ in Table 1. As the slepton mass gets

Table 1. 1σ (2σ) bounds from R_ℓ. The chargino sector parameters are specified in (3.1). The stop and sbottom parameters are specified in (3.5). The squarks of the first two generations are assumed to have the same mass as the sleptons

Slepton mass (GeV):	100	150	200	250	300
λ''_{313}, λ''_{323}	0.34(0.98)	0.36(1.04)	0.38(1.09)	0.39(1.14)	0.41(1.18)
λ''_{312}	0.31(0.91)	0.35(1.02)	0.39(1.12)	0.42(1.22)	0.46(1.32)
λ'_{131}, λ'_{132}	0.75(0.92)	0.83(1.03)	0.92(1.13)	1.0(1.24)	1.09(1.34)
λ'_{133}	0.85(1.05)	0.85(1.05)	0.84(1.04)	0.84(1.04)	0.84(1.04)
λ'_{231}, λ'_{232}	0.61(0.77)	0.68(0.85)	0.75(0.94)	0.82(1.03)	0.89(1.12)
λ'_{233}	0.70(0.88)	0.70(0.87)	0.69(0.87)	0.69(0.87)	0.69(0.86)
λ'_{331}, λ'_{332}	0.25(0.58)	0.28(0.65)	0.31(0.71)	0.34(0.78)	0.37(0.84)
λ'_{333}	0.29(0.66)	0.29(0.66)	0.29(0.66)	0.29(0.65)	0.29(0.65)

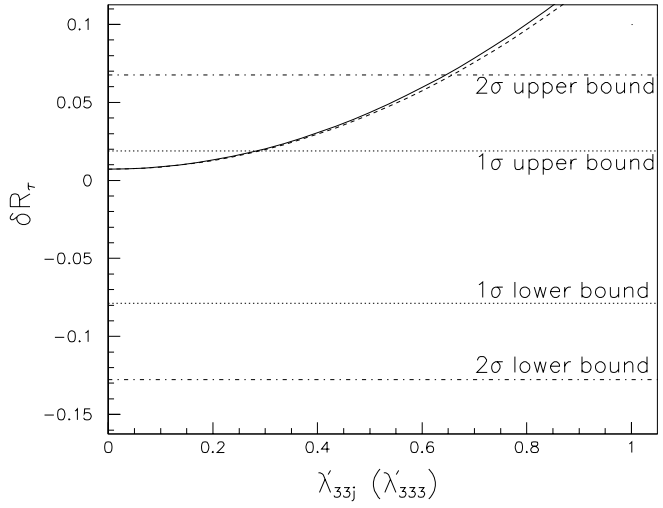

Fig. 10. δR_τ versus coupling strength. The solid curve is for λ'_{33j} ($j = 1$ or 2). The dashed curve is for λ'_{333}

larger, the contributions become smaller in magnitude and thus the bounds become weaker. Note that the bounds of λ'_{i33} ($i = 1, 2$ or 3) remain unchanged since their dominant contributions are from the top–sbottom loops, as shown in the last three diagrams of Fig. 5 with $j = k = 3$.

Since λ'_{i3k} contributions to R_{ℓ^i} have the same sign as the R conserving contributions while the λ''_{3jk} contributions to R_ℓ have the opposite sign, the inclusion of the R conserving contributions make the bounds stronger for λ'_{i3k} but weaker for λ''_{3jk}, compared to the case of neglecting R conserving contributions.

Among the L violating top quark couplings, λ'_{131}, λ'_{231} and λ'_{133} are already strongly constrained by atomic parity violation, ν_μ deep-inelastic scattering and the ν_e mass [8], respectively. The bounds are given by

$$\begin{aligned} &\lambda'_{131} < 0.035(2\sigma), \\ &\lambda'_{231} < 0.22(2\sigma), \\ &\lambda'_{133} < 0.0007(1\sigma), \end{aligned} \tag{3.8}$$

which are stronger than the R_ℓ bounds in Table 1. As for the other $\not{R}$ couplings listed in Table 1: none of them have been well constrained by other processes. Some theoretical bounds, by assuming the gauge group unification at $M_U = 2 \times 10^{16}$ GeV and the Yukawa couplings Y_t, Y_b and Y_τ to remain in the perturbative domain in the whole range up to M_U, give an upper bound of 1.25 [17]. So for these couplings the R_ℓ bounds are hitherto the strongest.

Note that we only presented some illustrative results for a limited set of SUSY parameters rather than scanning the whole SUSY parameter space allowed. It should be remarked that SUSY parameters in the MSSM are generally not well constrained experimentally at the present time. The only robust constraints are the LEP and Tevatron lower bounds on some of the sparticle masses [18, 19]. Therefore, the above SUSY parameter values used in our calculation are not the only choice. They are a set of representative values which are allowed by the current experimental bounds.

In the results in Table 1, we only varied the mass value of the slepton which is assumed to be degenerate with squarks in the first two generations. To see the effects of varying other SUSY parameters, we give the following comments instead of presenting lengthy numerical results.

(1) Dependence of the R conserving MSSM effects on $\tan\beta$. The R conserving MSSM effects are dominated by the $\tilde{t}_R$–b_L– Higgsino Yukawa coupling squared $\sim (M_t^2/M_W^2)(1 + \cot^2\beta)$, which is not sensitive to $\tan\beta$ in the range of intermediate and large $\tan\beta$. It is obvious that as $\tan\beta$ becomes lower than 1, which is disfavored by the existing experimental data, the R conserving MSSM effects will be greatly enhanced and thus the results will be very sensitive to $\tan\beta$. Of course, the R conserving MSSM effects also have other dependences on $\tan\beta$ through the chargino and stop masses and mixing angles. But in the range of intermediate and large $\tan\beta$ values, such a dependence is also mild.

(2) Dependence of the $\not{R}$ effects on $\tan\beta$. The λ'_{i33} contributions to $Z\ell^i\bar{\ell}^i$ through top quark loops shown in the last three diagrams of Fig. 5 involve sbottoms. The sbottom masses and mixing angle show a dependence on the $\tan\beta$ value. As $\tan\beta$ gets larger, the off-diagonal mass term $m_b(A_b\tilde{M} + \mu\tan\beta)$ increases and thus the mixing increases, which results in lighter $\tilde{b}_1$. Therefore, the λ'_{i33} contributions increase as $\tan\beta$ gets larger.

(3) As the mass parameters $\tilde{M}_Q$, $\tilde{M}_U$ and $\tilde{M}_D$ in the stop and sbottom get larger, stops and sbottoms will become heavier. As a result, the R conserving loop contribution to $Zb\bar{b}$, which involves stops, and the λ'_{i33} contribution to $Z\ell^i\bar{\ell}^i$, which involves sbottoms, will become smaller in magnitudes.
(4) If the mass parameters M, μ in the chargino sector get larger, the charginos will become heavier and the R conserving loop contribution to $Zb\bar{b}$, which involves charginos, will become smaller in magnitude.

4 Conclusion

In summary, we evaluated the quantum effects of the trilinear R-parity violating interactions on $Zb\bar{b}$ and $Z\ell\bar{\ell}$ couplings in the MSSM. We found the top quark $\not{R}$ couplings could give significant contributions through the top quark loops. When deriving the bounds from the R_b and R_ℓ data, we also took into account the loop contributions of R-parity conserving interactions, which are found to have the same sign as the λ'_{i3k} contributions and have a sign opposite to that of the λ''_{3jk} contributions. Therefore, the inclusion of the R-parity conserving contributions made the bounds stronger for λ'_{i3k}, but weaker for λ''_{3jk}, compared to the case of neglecting such R conserving contributions. The bounds from R_ℓ are found to be stronger than those from R_b and serve as the hitherto strongest bounds for some couplings.

Acknowledgements. The author thanks Ken-ichi Hikasa for useful discussions. This work is supported in part by the Grant-in-Aid for Scientific Research (No. 10640243) and Grant-in-Aid for JSPS Fellows (No. 97317) from the Japan Ministry of Education, Science, Sports, and Culture.

Appendix

The contribution factor $\Delta_R^{(\tilde{t}_L)}$ arises from the first three diagrams of Fig. 1, $\Delta_L^{(\tilde{t}_L)}$ from the middle three diagrams of Fig. 1 and $\Delta_L^{(\tilde{t}_R)}$ from the last three diagrams of Fig. 1, which are given by

$$\begin{aligned}\Delta_R^{(\tilde{t}_L)} = &-\frac{g^2}{16\pi^2}\left(\frac{M_b}{\sqrt{2}M_{\rm W}\cos\beta}\right)^2\\ &\times\Bigg\{-|U_{j2}|^2B_1(M_b,M_{\tilde{\chi}_j},M_{\tilde{t}_L})+U_{j2}^*U_{i2}\frac{O'^R_{ij}}{g^b_R}\\ &\times\Bigg[0.5-2C_{24}-M_Z^2(C_{11}-C_{12}+C_{21}-C_{23})\\ &+\frac{O'^L_{ij}}{O'^R_{ij}}M_{\tilde{\chi}_j}M_{\tilde{\chi}_i}C_0\Bigg](k,-p_{\bar{b}},M_{\tilde{\chi}_j},M_{\tilde{\chi}_i},M_{\tilde{t}_L})\\ &-\frac{g^t_L}{g^b_R}|U_{j2}|^2 2C_{24}(p_b,-k,M_{\tilde{\chi}_j},M_{\tilde{t}_L},M_{\tilde{t}_L})\Bigg\}, \quad (4.1)\end{aligned}$$

$$\begin{aligned}\Delta_L^{(\tilde{t}_L)} = &-\frac{g^2}{16\pi^2}\Bigg\{-|V_{j1}|^2B_1(M_b,M_{\tilde{\chi}_j},M_{\tilde{t}_L})+V_{j1}V_{i1}^*\frac{O'^L_{ij}}{g^b_L}\\ &\times\Bigg[0.5-2C_{24}-M_Z^2(C_{11}-C_{12}+C_{21}-C_{23})\\ &+\frac{O'^R_{ij}}{O'^L_{ij}}M_{\tilde{\chi}_j}M_{\tilde{\chi}_i}C_0\Bigg](k,-p_{\bar{b}},M_{\tilde{\chi}_j},M_{\tilde{\chi}_i},M_{\tilde{t}_L})\\ &-\frac{g^t_L}{g^b_R}|V_{j1}|^2 2C_{24}(p_b,-k,M_{\tilde{\chi}_j},M_{\tilde{t}_L},M_{\tilde{t}_L})\Bigg\}, \quad (4.2)\end{aligned}$$

$$\begin{aligned}\Delta_L^{(\tilde{t}_R)} = &-\frac{g^2}{16\pi^2}\left(\frac{M_t}{\sqrt{2}M_{\rm W}\sin\beta}\right)^2\Bigg\{-|V_{j2}|^2B_1\\ &\times(M_b,M_{\tilde{\chi}_j},M_{\tilde{t}_R})+V_{j2}V_{i2}^*\frac{O'^L_{ij}}{g^b_L}\Bigg[0.5-2C_{24}-M_Z^2\\ &\times(C_{11}-C_{12}+C_{21}-C_{23})+\frac{O'^R_{ij}}{O'^L_{ij}}M_{\tilde{\chi}_j}M_{\tilde{\chi}_i}C_0\Bigg]\\ &\times(k,-p_{\bar{b}},M_{\tilde{\chi}_j},M_{\tilde{\chi}_i},M_{\tilde{t}_R})-\frac{g^t_R}{g^b_R}|V_{j2}|^2 2C_{24}\\ &\times(p_b,-k,M_{\tilde{\chi}_j},M_{\tilde{t}_R},M_{\tilde{t}_R})\Bigg\}. \quad (4.3)\end{aligned}$$

Here the functions B_1 and C_{ij}, C_0 are 2- and 3-point Feynman integrals defined in [20], and their functional dependences are indicated in the bracket following them with k, p_b and $p_{\bar{b}}$ being the momentum of Z-boson, b and $\bar{b}$, respectively. The O'^L_{ij} and O'^R_{ij} are defined by $O'^L_{ij} = -V_{i1}V_{j1}^* - V_{i2}V_{j2}^*/2 + \delta_{ij}\sin^2\theta_{\rm W}$ and $O'^R_{ij} = -U_{i1}^*Uj1 - U_{i2}^*U_{j2}/2 + \delta_{ij}\sin^2\theta_{\rm W}$, respectively. The unitary matrix elements U_{ij} and V_{ij}, and the chargino masses $\tilde{M}_j$ depend on the parameters M, μ and $\tan\beta$ via (c18)–(c21) of [2]. Here we defined $\tan\beta = v_2/v_1$ with v_2 (v_1) being the VEV of the Higgs doublet giving up-type (down-type) quark masses, so θ_v in [2] should be substituted by $\pi/2-\beta$. M is the $SU(2)$ gaugino masses and μ is the coefficient of the H_1H_2 mixing term in the superpotential.

The contribution of Fig. 2 to $Zb_R\bar{b}_R$ coupling is given by

$$\begin{aligned}\Delta_R^{(\lambda''_{ij3})} = &-|\lambda''_{ij3}|^2\frac{f_c}{16\pi^2}\Bigg\{-B_1(M_b,M_{d^j},M_{\tilde{u}^i_R})\\ &-B_1(M_b,M_{u^i},M_{\tilde{d}^j_R})+2\frac{g^{\tilde{u}^i_R}_R}{g^b_R}\\ &\times C_{24}(p_b,-k,M_{d^j},M_{\tilde{u}^i_R},M_{\tilde{u}^i_R})+2\frac{g^{\tilde{d}^j_R}_R}{g^b_R}\\ &\times C_{24}(p_b,-k,M_{u^i},M_{\tilde{d}^j_R},M_{\tilde{d}^j_R})-\frac{g^{d^j}_R}{g^b_R}\\ &\times\Bigg[0.5-2C_{24}-M_Z^2(C_{11}-C_{12}+C_{21}-C_{23})\end{aligned}$$

$$+\frac{g_L^{d^j}}{g_R^{d^j}}M_{d^j}^2C_0\Big](k,-p_{\bar{b}},M_{d^j},M_{d^j},M_{\tilde{u}_R^i})-\frac{g_R^{u^i}}{g_R^b}$$
$$\times\Big[0.5-2C_{24}-M_Z^2(C_{11}-C_{12}+C_{21}-C_{23})$$
$$+\frac{g_L^{u^i}}{g_R^{u^i}}M_{u^i}^2C_0\Big](k,-p_{\bar{b}},M_{u^i},M_{u^i},M_{\tilde{d}_R^j})\Big\}. \quad (4.4)$$

Here, for a field f, the left- and right-handed couplings are defined by $g_L^f=I_3^f-e_fs_{\rm W}^2$ and $g_R^f=-e_fs_{\rm W}^2$ with e_f being the electric charge in the unit of e, and $I_3^f=\pm1/2$ the corresponding third components of the weak isospin. $f_c=2$ is a color factor.

The contribution of Fig. 3 to the $Zb_R\bar{b}_R$ coupling is found to be

$$\Delta_R^{(\lambda'_{ij3})}=|\lambda'_{ij3}|^2\frac{1}{16\pi^2}\sum_{f,\tilde{f}}\Big\{B_1(M_b,M_f,M_{\tilde{f}})+2\frac{g_L^{\tilde{f}}}{g_R^b}$$
$$\times C_{24}(p_b,-k,M_f,M_{\tilde{f}},M_{\tilde{f}})-\frac{g_L^f}{g_R^b}\Big[0.5-2C_{24}$$
$$-M_Z^2(C_{11}-C_{12}+C_{21}-C_{23})+\frac{g_R^f}{g_L^f}M_f^2C_0\Big]$$
$$\times(k,-p_{\bar{b}},M_f,M_f,M_{\tilde{f}})\Big\}, \quad (4.5)$$

where the sum is performed over

$$(f,\tilde{f})=\begin{cases}(d^j,\tilde{\nu}_L^i),\\(\nu^i,\tilde{d}_L^j),\\(u^j,\tilde{e}_L^i),\\(e^i,\tilde{u}_L^j).\end{cases} \quad (4.6)$$

The contribution of Fig. 4 to $Zb_L\bar{b}_L$ coupling is given by

$$\Delta_L^{(\lambda'_{i3k})}=|\lambda'_{i3k}|^2\frac{1}{16\pi^2}\Big\{B_1(M_b,M_{d^k},M_{\tilde{\nu}^i})$$
$$+B_1(M_b,0,M_{\tilde{d}_R^k})$$
$$-2\frac{g_L^{\tilde{\nu}^i}}{g_L^b}C_{24}(-p_b,k,M_{d^k},M_{\tilde{\nu}^i},M_{\tilde{\nu}^i})$$
$$+2\frac{g_R^{\tilde{d}^k}}{g_L^b}C_{24}(p_b,-k,0,M_{\tilde{d}_R^k},M_{\tilde{d}_R^k})$$
$$-\frac{g_R^{d^k}}{g_L^b}\left[0.5-2C_{24}-M_Z^2(C_{11}-C_{12}+C_{21}\right.$$
$$\left.-C_{23})\right](-k,p_{\bar{b}},M_{d^k},M_{d^k},M_{\tilde{\nu}^i})$$
$$+\frac{g_L^{\nu^i}}{g_L^b}\left[0.5-2C_{24}-M_Z^2(C_{11}-C_{12}+C_{21}\right.$$
$$\left.-C_{23})\right](k,-p_{\bar{b}},0,0,M_{\tilde{d}_R^k})\Big\}. \quad (4.7)$$

References

1. For example, see K. Whisnant, J.M. Yang, B.-L. Young, X. Zhang, Phys. Rev. D **56**, 467 (1997); J.M. Yang, B.-L. Young, Phys. Rev. D **56**, 5907 (1997); G.J. Gounaris, D.T. Papadamou, F.M. Renard, Z. Phys. C **76**, 333 (1997); G.J. Gounaris, F.M. Renard, C. Verzegnassi, Phys. Rev. D **52**, 451 (1995); For early references, see, e.g., C.J.C. Burgess, H.J. Schnitzer, Nucl. Phys. B **228**, 454 (1983); C.N. Leung, S.T. Love, S. Rao, Z. Phys. C **31**, 433 (1986); W. Buchmuller, D. Wyler, Nucl. Phys. B **268**, 621 (1986)
2. For an introduction to the phenomenology of the MSSM, see H. Haber, G.L. Kane, Phys. Rept. **117**, 75 (1985)
3. For some early references on the phenomenology of R violating supersymmetry, see L. Hall, M. Suzuki, Nucl. Phys. B **231**, 419 (1984); J. Ellis et al., Phys. Lett. B **150**, 142 (1985); G. Ross, J. Valle, Phys. Lett. B **151**, 375 (1985); S. Dawson, Nucl. Phys. B **261**, 297 (1985); R. Barbieri, A. Masiero, Nucl. Phys. B **267**, 679 (1986); H. Dreiner, G.G. Ross, Nucl. Phys. B **365**, 597 (1991); J. Butterworth, H. Dreiner, Nucl. Phys. B **397**, 3 (1993)
4. H1 Collab., C. Adloff et al., DESY 97-024 (1997); ZEUS Collab., J. Breitweg et al., DESY 97-025 (1997)
5. Super Kamiokande Collaboration, Y. Fukuda et al., Phys. Rev. Lett. **81**, 1562 (1998); T. Kajita, talk at Neutrino '98, Takayama, Japan, June, 1998; For recent reviews, see J.M. Conrad, summary talk at ICHEP '98, hep-ex/981109; R.D. Peccei, hep-ph/9906509; H. Robertson, talk presented at Lepton-Photon'99; the transparencies are available at http://www-sldnt.slac.stanford.edu/lp99/pdf/33.pdf
6. For the phenomenology of R-violation in some decays, see V. Barger, G.F. Giudice, T. Han, Phys. Rev. D **40**, 2978 (1989); K. Agashe, M. Graesser, Phys. Rev. D **54**, 4445 (1996); F. Zwirner, Phys. Lett. B **132**, 103 (1983); R.N. Mohapatra, Phys. Rev. D **34**, 3457 (1986); M. Hirsch, H. Kleingrothaus, S.G. Kovalenko, Phys. Rev. Lett. **75**, 17 (1995); K.S. Babu, R.N. Mohapatra, Phys. Rev. Lett. **75**, 2276 (1995); G. Bhattacharyya, D. Choudhury, Mod. Phys. Lett. A **10**, 1699 (1995); D.E. Kaplan, hep-ph/9703347; J. Jang, J.K. Kim, J.S. Lee, Phys. Rev. D **55**, 7296 (1997); G. Bhattacharyya, A. Raychaudhuri, Phys. Rev. D **57**, 3837 (1998); J.M. Yang, B.-L. Young, X. Zhang, Phys. Rev. D **58**, 055001 (1998); T.-F. Feng, hep-ph/9806505; S. Bar-Shalom, G. Eilam, A. Soni, hep-ph/9812518
7. For some recent studies of collider phenomenology of R-violation, see J. Erler, J.L. Feng, N. Polonsky, Phys. Rev. Lett. **78**, 3063 (1997); A. Datta, J.M. Yang, B.-L. Young, X. Zhang, Phys. Rev. D **56**, 3107 (1997); R.J. Oakes, et al., Phys. Rev. D **57**, 534 (1998); J.L. Feng, J.F. Gunion, T. Han, Phys. Rev. D **58**, 071701 (1998); D.K. Ghosh, S. Raychaudhuri, K. Sridhar, Phys. Lett. B **396**, 177 (1997); S. Bar-Shalom, G. Eilam, A. Soni, Phys. Rev. Lett. **80**, 4629 (1998); Phys. Rev. D **59**, 055012 (1999); S. Bar-Shalom, G. Eilam, J. Wudka, A. Soni, Phys. Rev. D **59**, 035010 (1999); B.C. Allanach, H. Dreiner, P. Morawitz, M.D. Williams, Phys. Lett. B **420**, 307 (1998); E. Perez, Y. Sirois, H. Dreiner, hep-ph/9703444
8. For a review of current bounds, see H. Dreiner, hep-ph/9707435, published in Perspectives on Supersymmetry, edited by G.L. Kane; R. Barbier, et al., hep-ph/9810232; G. Bhattacharyya, hep-ph/9709395; P. Roy, hep-ph/9712520
9. T. Appelquist, J. Carazzone, Phys. Rev. D **11**, 2856 (1975)

10. G. Bhattacharyya, J. Ellis, K. Sridhar, Mod. Phys. Lett. A **10**, 1583 (1995); G. Bhattacharyya, D. Choudhury, K. Sridhar, Phys. Lett. B **355**, 193 (1995)
11. The LEP Collaborations, CERN-EP-2000-016; M. Swartz, talk at Lepton–Photon'99
12. A. Joshipura, M. Nowakowski, Phys. Rev. D **51**, 5271 (1995); F. de Campos, M.A. Garcia-Jareno, A.S. Joshipura, J. Rosiek, J.W.F. Valle, Nucl. Phys. B **451**, 3 (1995); V. Barger, M.S. Berger, R.J.N. Phillips, T. Wöhrmann, Phys. Rev. D **53**, 6407 (1996)
13. A. Djouadi, G. Girardi, C. Verzegnassi, W. Hollik, F.M. Renard, Nucl. Phys. B **349**, 48 (1991); M. Boulware, D. Finnell, Phys. Rev. D **44**, 2054 (1991); C.S. Li, J.M. Yang, B.Q. Hu, Commun. Theor. Phys. **20**, 213 (1993)
14. J. Ellis, S. Rudaz, Phys. Lett. B **128**, 248 (1983); A. Bouquet, J. Kaplan, C. Savoy, Nucl. Phys. B **262**, 299 (1985)
15. See, e.g., the L3 collaboration, hep-ex/0012017
16. See, e.g, A. Czarnecki, W. J. Marciano, hep-ph/0102122
17. B. Brahmachari, P. Roy, Phys. Rev. D **50**, 39 (1994)
18. Joint SUSY Working Group of LEP, http://www.cern.ch/lepsusy/
19. CDF collaboration, Phys. Rev. D 56, R1357 (1997); D0 Collaboration, Phys. Rev. Lett. **76**, 2222 (1996)
20. G. Passarino, M. Veltman, Nucl. Phys. B **160**, 151 (1979)